Tianjin Daxue Xuebao (Ziran Kexue yu Gongcheng Jishu Ban)/
Journal of Tianjin University Science and Technology
ISSN (Online): 0493-2137
E-Publication: Online Open Access
Vol:54 Issue:04:2021
DOI 10.17605/OSF.IO/G3678

DENOISING OF MR IMAGES USING REFORMED STRUCTURAL LOSS BASED 3D MULTI-SCALE DEEP NEURAL NETWORK (RSLM-DNN-3D)

A. Aaisha Nazleem[1], Dr. S. S. Sujatha[2]
[1]Research Scholar, Reg No (17233152162001) S.T. Hindu College, Nagarcoil
[2]Associate Professor, Department of Computer Science S.T. Hindu College, Nagarcoil

Abstract:
Noise reduction or denoising of images will help in getting true images from noisy images. The differentiations of noise from other part of the images are difficult because edge and texture are also having high frequency as like noise. This work addresses the issue of denoising in Magnetic Resonance Imaging (MRI). This work proposes a new technique known as Reformed Structural Loss based 3D Multi-scale Deep Neural Network (RSLM-DNN-3D) which is a variation of Generative Adversarial Network (GAN). A generator and a discriminator circuit help the work to reduce the noise. In order to preserve more structural information, a reformed model of multi scale 3D CNN model is proposed as Generator of this GAN framework. The proposed work gives good results when compared to Wasserstein Generative Adversarial Network (WGAN) and CNN based approach.

1. Introduction

Magnetic Resonance Imaging (MRI) [1], a prominent technology which gives the high detailed information about the human living tissues such as changes in pathological and physiological with imaging. It gives the raw information of the concerned body parts which are sampled directly. The MRI images give two dimensional section of body with corresponding position, contrast and orientation of tissues. Different standards are used for the sampling which may lead to undersampling .This undersampling suffers the penalty of signal to noise ratio (SNR). Low SNR which is a resultant of undersampling will lead to corrupting the images visually and addition of noise to the images. Proper denoising technique should be used for removing the noise. Because of the ease of usage different applications use MRI in various applications like cardiac imaging, brain imaging, dynamic imaging of liver, musculoskeletal and reticuloendothelial systems etc. Since the MRI processing relies on prior processed data, noise in the data will affect the process badly. Also, the occurrence of noise is unavoidable because it usually happens in MRI when it is captured, processed or stored. So reducing and removing of noise becomes an inevitable one in this field [2]. Denoising is the technique used for this. This technique has lot of research scope because lack of optimized noise removal may lead to blurring or introduction of other problems in images. Usually the reconstruction of MRI is done by using inverse DFT (Discrete Fourier Transform), where the information will be available in both real and imaginary part. Gaussian noise [3] will be there in both of these channels.

MRI signal's magnitude, which is derived by the two different Gaussian variables is used for analysis of the images. So it leads to Rician distribution [4]. The denoising techniques may be done during the acquisition or post acquisition of images. The denoising after post acquisition tries to reduce the power of noise by maintaining the resolution of the original image.

2. Related Work

Many researches have worked on denoising techniques. A neutrosophicset approach was proposed by Mohan et al [5], which is based on wiener filtering. Another work [6] was proposed the denoising by non-locl mean filter and anisotropic diffusion filter. Many other works were also donefordenoising techniques [7-13]. MRI denoising techniques may be proposed based on three sectors like the methods to work in spatial domain, which works in

Tianjin Daxue Xuebao (Ziran Kexue yu Gongcheng Jishu Ban)/
Journal of Tianjin University Science and Technology
ISSN (Online): 0493-2137
E-Publication: Online Open Access
Vol:54 Issue:04:2021
DOI 10.17605/OSF.IO/G3678

transformed domain and which work based on the statistical details of the signals by considering the parameters like improvement of performance, reducing the computational time and cost [14-17]. Markov random field (MRF) based methods were proposed [18-19], which works in spatial domain and finds the inter-relation between the pixels. It works on the image for preserving the edges and structures which helps to regulate the noise and to smooth the image signals based on the local characteristics. Like other fields, medical imaging also started to use deep learning [20-24] for finding solutions to its problems. Different applications which are using deep learning in medical field are noise reduction[24], image classification [25], image registration [26-27] and brain image segmentation [28].

Residual Encoder-Decoder Convolutional Neural Network (REN-CNN) [29] is a method used for predicting and reducing noises in LDCT images. Though the noises are reduced to a larger extent by this method, blurring may happen because of the minimized mean square error between the output image with the corresponding NDCT images. Blurring in the images are greatly reduced by introducing generative adversarial network (GAN) [30], where two networks are used: generator and discriminator. The generator captures the distribution of real data and discriminator discriminates between distributed data and synthetic data. Original GAN suffers from non-convergence and unstable training. In this authors have used Jensen-Shannon (JS) divergence for measuring the similarity. Wasserstein distance [31] was introduced to overcome this demerit.

Many researches [35-36] were started in working with losses. For considering the chances of getting losses in denoising techniques and for reducing it, different directions on research were done. Perceptual loss [34] is a loss which captures the effect of denoisingby finding the difference of reference image with denoised image. The denoising of clinical images gives better result when it is worked with perceptual loss. But perceptual loss based work does not work well when it is applied to traditional images because the evaluation is done generic ways.

To address this issue different variations of Generative Adversarial Networks (GAN) were used. Chenyuet. Al. [32] used Multi-scale Generative Adversarial Network (SMGAN) by considering structural sensitivity of the images. Based on this work, the proposed work also considers the sensitiveness in structure of the images in terms of various losses like structural loss, L1 loss and Adversarial loss.

Organization of this paper isas follows: Section III gives the proposed work where the proposed network is explained along with details of losses. Section IV gives theexperimentalanalysis. Section V discusses gives the concluding remarks.

3. Proposed Work

This paper proposes a new architecture called RSLM-DNN-3D (Reformed Structural Loss based 3D Multi-scale Deep Neural Network). This work is based on SMGAN [32], the proposed network gives structurally-sensitive loss which influences three losses: perceptually-favorable structural loss, pixel-wise L1 loss and adversarial loss. The proposed network comprised of a 3D generator and 3D discriminator.

Let x and y be the noise free MRI (NFMRI) image and noisy MRI image (NMRI) respectively with H, W and D where H is height, W is width and D is number of slices. The relationship between these images is:

$$y = T(\mathrm{x}) + \varepsilon \quad (1)$$

Where T is a generic noising process which degrades the image.H, WandD are height, widthand depth respectively. The aim of denoising is to extract the desired image x from the noisy image y. This can be done by solving inverse problem as $T^t = T^{-1}$ which will help to retrieve the denoised image. The output will be $T^t y \simeq \dot{\mathrm{x}} \simeq \mathrm{x}$. Figure 1 gives the proposed architecture. It has three parts: a generator, Structurally-Sensitive loss (SSL) functionand discriminator. The noisy MRI imageimage is converted into noise free MRI image using G.

Tianjin Daxue Xuebao (Ziran Kexue yu Gongcheng Jishu Ban)/
Journal of Tianjin University Science and Technology
ISSN (Online): 0493-2137
E-Publication: Online Open Access
Vol:54 Issue:04:2021
DOI 10.17605/OSF.IO/G3678

The dissimilarity in structural sensitiveness between both is calculated by SSL. D is used to differentiate the synthetic results from real one. Based on the outcome of G and D, they compete each other in improving the results. The following part of this section describes about the structure and functionality of G, SSL and D.

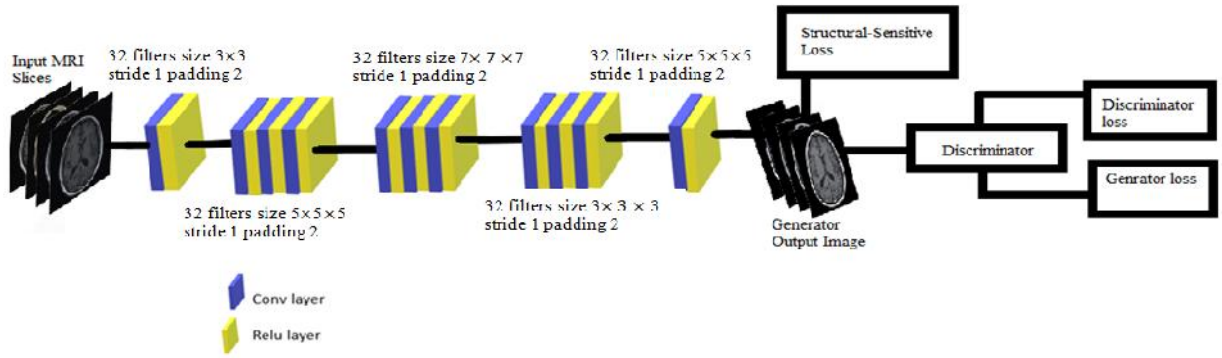

Fig. 1: The overall structure of the proposed network.

a. 3D Multi Scale CNN Generator:

The generator G is used for synthesizing the new data from previously available data. The proposed network uses the generator with layers. All the layers have 32 filters. The layers are split into five stages. The first stage with one convolutional layers has 3X3X1 filters with padding of 1. The second stage with three convolutionallayers has 5X5X5filters with padding 2. The third stage with three convolutional layers has 7X7X7 filters with padding 3. The fourthconvolutional layer has 3X3X3 filters with padding of 1. Last convolutional layer has 3X3X1 filters with padding of 1. The Rectified Linear Unit (ReLU) layer is used after each Conv layer.

b. Discriminator

This work uses six convolutional layers which have 3 x 3 kernel sizewith filters 64, 64, 128, 128, 256, and 256. Two fully connected layers are used after the convolutional layers. First fully connected layer produces 1024 feature maps which isfollowed by a leaky ReLU layer. Second fully convolutional layer gives 1 feature map which is followed by another leaky ReLU layer.

c. Loss Functions for Noise Reduction

The loss in noise reduction in the proposed work may happen due to L1 loss, adversarial loss and Structural Loss. The different losses should be evaluated properly for identifying the reasons for loss and to avoid it. L1 loss is based on mean. Blurring will not happen much in L1 loss. But the fact is it suffers from blocky structures in the image. Adversarial loss is calculated by Wasserstein distance [33]. Structural loss is calculated by multi-scale structural similarity index and structural similarity index. Structural loss can be easily propagated backwards and correct the image.

The L1 loss can be calculated by using H (height), W(width), D(depth) of a 3D image patch as,

$$L_{1=\frac{1}{HWD}|G(y)-\mathrm{x}|'} \quad (2)$$

Wheregold-standard (NFMRI) is given by x the output generated from source image is given by G(y). The adversarial loss is calculated by taking values of z which is G(y) for brevity and ẍ which issampled uniformly through the straight line between the points which are sampled from G and corresponding NFMRI images as

$$L_{adv} = -E[D(\ddot{\mathrm{x}})] + \mathrm{E}[D(\mathrm{z})] + \lambda \mathrm{E}|(||\nabla_{\mathrm{x}} D(\ddot{\mathrm{x}})||_2 - 1)^2| \quad (3)$$

Tianjin Daxue Xuebao (Ziran Kexue yu Gongcheng Jishu Ban)/
Journal of Tianjin University Science and Technology
ISSN (Online): 0493-2137
E-Publication: Online Open Access
Vol:54 Issue:04:2021

d. Structurally-Sensitive Loss (SSL) Function

Structurally-Sensitive Loss (SSL) SSL function [32] is used to find the differences in patch-wise. 3D SSL function is used in this work the difference of 3D output and 3D NFMRI image. This information is used for updating network parameter. .

The structural loss is calculated by using C1 and C2 which are constants. μ_x,μ_z, σ_x, σ_z andσ_{xz}denote the mean of image x, mean of image z, standard deviation of x, standard deviation of z and cross-covariance of the images x and z. x is the image and z is the corresponding NFMRI image. structural similarity index (SSIM) can be calculated as

$$\text{SSIM}(x,y)=\frac{2\mu_x\mu_z+C_1}{\mu_x{}^2+\mu_z{}^2+C_1}*\frac{2\sigma_{xz}+C_2}{\sigma_x{}^2+\sigma_z{}^2+C_2}=l(x,z)*cs(x,z). \quad (4)$$

From the SSIM measure, we can calculate multi-scale structural similarity index (MS-SSIM) as $MS-SSIM(x,z)=\prod_{i=1}^{M}SSIM(x_i,z_i)$. From these data, SL can be calculated as$L_{SL}=1-MS-SSIM(x,z)$

e. Objective Function

The L_1loss will have suppressed noise and improved SNR (Signal to Noise Ratio). But it makes blurring in the image. The structural loss will not make blurring and gives good resolution images. To get the advantages of these two losses Structural Sensitive Loss (SSL) is calculated by using τ which is the weighting factor as,

$$L_{SSL}=\tau*L_{SL}+(1-\tau)*L_1. \quad (5)$$

The τ is used to balance the L_1 loss and structural loss. Because of the fact that L_{SSL} suffers from missing of few diagnostic features, adversarial loss also need to be incorporated into it. since the adversarial loss can accommodate both structural and textural features. It can be represented as,

$$L_{obj}=L_{SSL}+\beta*L_{adv} \quad (6)$$

The weight of the adversarial loss is represented by β. The output image is compared with the target image based on these losses. This loss is propagated backwards for getting optimized result.

4. Experimental Analysis

The proposed network is evaluated experimentally. It takes a dataset, which is obtained from [37],brats17 challenge. Which consist of multimodal MRI scans of glioblastoma (GBM/HGG) and lower grade glioma (LGG), with pathologically confirmed diagnosis and provided as the training, validation and testing data. From this T1cMRI brain DICOM image of 20patientsis used for this analysis. Where each patient set consist of 154 slices. In this dataset, the 70% data are randomly selected for training set and the 30% data are randomly selected for testing.

Peak signal-to-noise ratio (PSNR) is used to evaluate the performance of the work. It gives the comparison between two images. This ratio provides the quality measurement of the denoised image with the original image. The original image is meant to be the ideal image.

PSNR can be calculated as follows:

$$\text{PSNR} = 10\log_{10}(\text{MAX}^2/\text{MSE}) \quad (7)$$

Where MAXis the maximum intensity value of the image and MSE is the Mean Square Error. The SSIM index is used as an another measure to calculate the performance which is calculated on different windows of the image. SSIMindex between the two windows with common size $N\times N$ can be calculated as:

$$\text{SSIM}(x,y)=\frac{(2\mu_x\mu_y+c_1)(2\sigma_{xy}+c_2)}{(\mu_x^2+\mu_y^1+c_1)(\sigma_x^2+\sigma_y^2+c_2)} \quad (8)$$

Normalized Cross-correlation (NCC) is another m[redacted]e to be calculated [redacted]image which can be calculated using the equation.

$$\text{NCC}(\text{Image1},\text{Image2})=\frac{1}{N\sigma_1\sigma_2}\sum_{x,y}(\text{Image1}(x,y)-[\text{redacted}])x(\text{Image2}(x,y)-[\text{redacted}]2) \quad (9)$$

Tianjin Daxue Xuebao (Ziran Kexue yu Gongcheng Jishu Ban)/
Journal of Tianjin University Science and Technology
ISSN (Online): 0493-2137
E-Publication: Online Open Access
Vol:54 Issue:04:2021

Where Image 1 and Image 2 are NFMRI and NMRI, N is total number of pixels in the image ,$\sigma_{1 \text{ and }} \sigma_2$ are standard deviation values.

Input Noise Image	De-noised Image	PSNR
	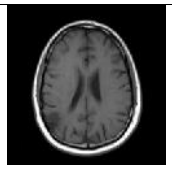	44.51
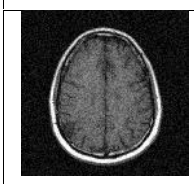	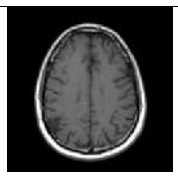	44.96
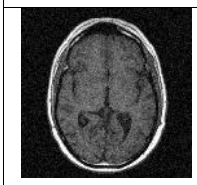	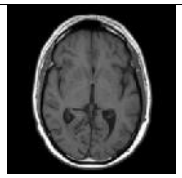	44.55
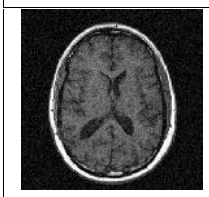	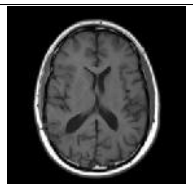	43.76

Fig. 1: Sanple Denoised MRI slices using the proposed RSLM-DNN-3D

Figure 1 shows some of sample denoised MRI slices using the proposed method and its corresponding PSNR values. Following Table 1 shows that the performance of SMGAN-3D, WGAN, CNN_L1 and RSLM-DNN-3D based on the PSNR value for the slice of T1 weighted MRI DICOM images. The proposed work gives better result (+3) than SMGAN-3D, +4.6 than WGAN and +6.6 than CNN_L1. Figure 2 gives the comparison of PSNR value for the slice of T1 weighted MRI DICOM images of proposed work with previous works

Table.1 Performance of SMGAN-3D, WGAN, CNN_L1and RSLM-DNN-3Dbased on the PSNR value for the slice of T1 weighted MRI DICOM images.

Patient ID	1	2	3	4	5	6	Mean
SMGAN-3D	42.82	39.03	41.8	40.47	41.55	41.63	41.21667
WGAN	40.78	37.45	39.02	38.69	40.01	40.59	39.42333
CNN_L1	37.56	38.27	37.94	36.72	37.09	37.61	37.5316
RSLM-DNN-3D	44.51	44.96	44.55	43.76	43.73	43.96	44.245

Fig. 2: Comparison ofPSNR value for the slice of T1 weighted MRI DICOM images of proposed work with previous works

Tianjin Daxue Xuebao (Ziran Kexue yu Gongcheng Jishu Ban)/
Journal of Tianjin University Science and Technology
ISSN (Online): 0493-2137
E-Publication: Online Open Access
Vol:54 Issue:04:2021

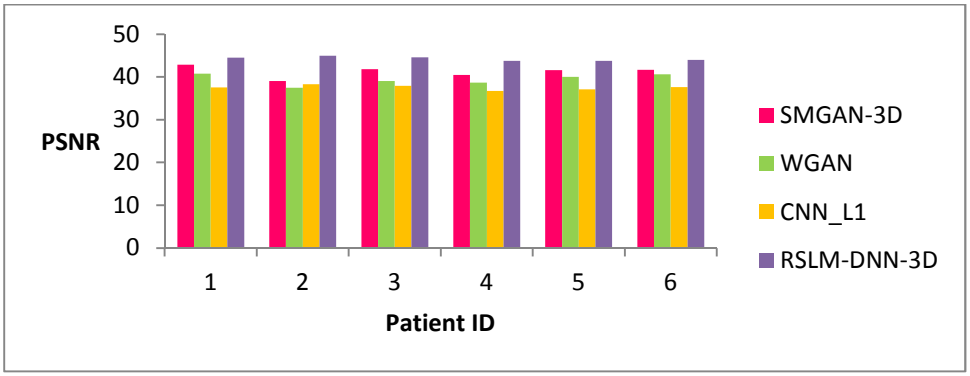

Table2 shows that the performance of SMGAN-3D, WGAN, CNN_L1 and RSLM-DNN-3D based on the SSIM value for the slice of T1 weighted MRI DICOM images and Figure 3 gives the diagrammatic representation of the same. From these it is clear that the proposed work outperforms other previous works.

Table.2 Performance analysis of SMGAN-3D, WGAN, CNN_L1 and RSLM-DNN-3Dbased on the SSIM value for the slice of T1 weighted MRI DICOM images.

Patient ID	**1**	**2**	**3**	**4**	**5**	**6**	**Mean**
SMGAN-3D	0.9802	0.97865	0.97662	0.964	0.962	0.9765	0.972995
WGAN	0.9694	0.967	0.9622	0.9532	0.9452	0.9595	0.95941667
CNN_L1	0.967	0.9601	0.95	0.944	0.94	0.954	0.95251667
RSLM-DNN-3D	0.99	0.9902	0.9899	0.983	0.984	0.98934	0.98774

Fig. 3: Comparison ofSSIM values for the slice of T1 weighted MRI DICOM images of various works

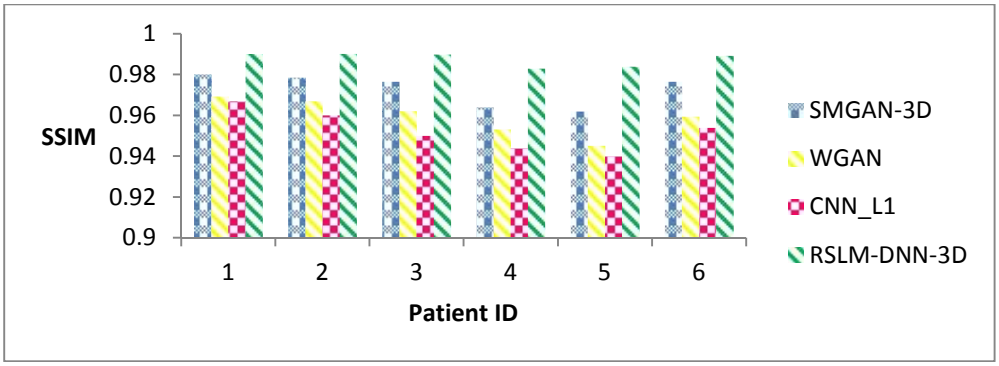

Table.3shows that the performance of SMGAN-3D, WGAN, CNN_L1 and RSLM-DNN-3D based on the NCC value for the slice of T1 weighted MRI DICOM images and Figure 4 gives the diagrammatic representation of the same which show the better performance of the proposed work when compared to the other previous works

Table.3 Performance of SMGAN-3D, WGAN, CNN_L1and RSLM-DNN-3Dbased on the NCC value for the slice of T1 weighted MRI DICOM images.

Tianjin Daxue Xuebao (Ziran Kexue yu Gongcheng Jishu Ban)/
Journal of Tianjin University Science and Technology
ISSN (Online): 0493-2137
E-Publication: Online Open Access
Vol:54 Issue:04:2021

Patient ID	1	2	3	4	5	6	Mean
SMGAN-3D	0.974	0.98934	0.9734	0.9688	0.9688	0.9733	0.97460667
WGAN	0.963	0.97633	0.9652	0.9633	0.9433	0.9599	0.96183833
CNN_L1	0.961	0.9574	0.9491	0.9545	0.939	0.9536	0.95243333
RSLM-DNN-3D	0.988	0.993	0.989	0.9878	0.978	0.982	0.9863

Fig. 4. Performance comparison of NCC of SMGAN-3D, WGAN, CNN_L1and RSLM-DNN-3D.

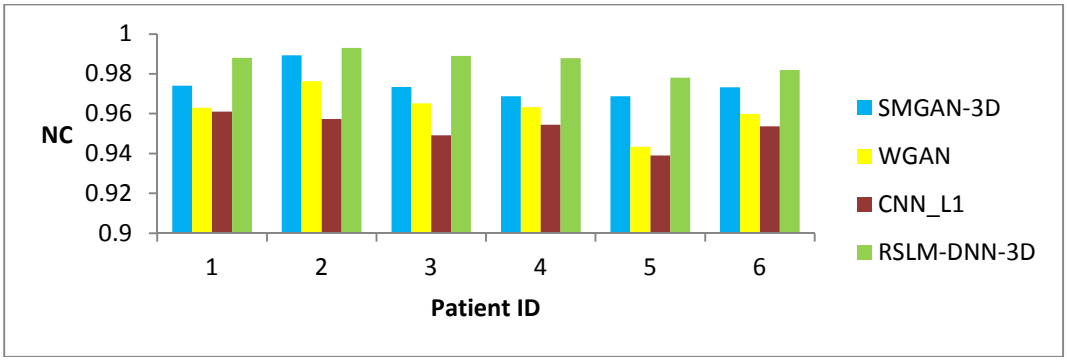

The structural sensitiveness of the images gives better information to work on with various losses. So the denoising of the images is achieved well by the proposed work.

5. Conclusion

Deep learning techniques work well for almost all the applications because of its ability to re-learn and correct itself. The proposed network for denosing of MRI image gives good result than many of the previous works because of its ability to grab the dissimilarity in structure. Also generator and discriminator compete each other well to reduce the difference and thereby improve the performance of the output. This work can be further improved by designing a generator with appropriate discriminator with adaptive loss structure to preserve sensitive data in some more extend form.

References

[1] Wright G, 1997. “Magnetic Resonance Imaging”, IEEE Signal Process Mag. 14, pp. 56-66.
[2] Rajeesh J, Moni RS, Palanikumar S, Gopalakrishnan T. Noise reduction in magnetic resonance images using wave atom shrinkage. International Journal of Image Processing (IJIP). 2010;4(2):131-141
[3] Henkelman R.M, 1985. “Measurement of signal intensities in the presence of noise in MR images”, Med. Phys.12, pp. 232–233.
[4] Gudbjartsson H. and Patz S, 1995. “The Rician distribution of noisy MRI data”, Magn.Reson. Med. 34, pp. 910–914
[5] Mohan J, Krishnaveni V, Guo Y and Kanchana J, 2012. “MRI denoising based on neutrosophic wiener filtering”, Proc. IEEE International Conference on Imaging Systems and Techniques (IST 2012) Manchester, United Kingdom.
[6] Mohan J, Krishnaveni V and Guo Y, 2012. “Performance analysis of neutrosophic set approach of median filtering for MRI denoising”, Int. J Elec. &Commn. Engg& Tech. 3, pp. 148-163.
[7] Phophalia A, Rajwade A, Mitra SK. Rough set based image de-noising for brain MR images. Signal Processing. 2014;103(2014):24-35
[8] Rahmat R, Malik AS, Kamel N. Comparison of LULU and median filter for image denoising. International Journal of Computer and Electrical Engineering. 2013;5(6)

[9] Isa IS, Sulaiman SN, Mustapha M, Darus S. Evaluating de-noising performances of fundamental filters for T2-weighted MRI images. 19th International Conference on Knowledge Based and Intelligent Information and Engineering Systems.Procedia Computer Science. 2015;60:760-768
[10] Zhang M, Gunturk BK. Multi resolution bilateral filtering for image de-noising. IEEE Transactions on Image Processing. 2008;17(12):2324-2333
[11] Akar SA. Determination of optimal parameters for bilateral filter in brain MRimagedenoising.Applied Soft Computing. 2016;43:87-96
[12] Lakshmi Devasena C, Hemalatha M. Noise removal in magnetic resonance images using hybrid KSL filtering technique. International Journal of Computer Applications (0975-8887);27(8):2011
[13] Dey N, Ashour AS, Beagum S, SifakiPistola D, Gospodinov M, Gospodinova E, Tavares RS. Parameter optimization for local polynomial approximation based intersection confidence interval filter using genetic algorithm: An application for brain MRI image denoising. Journal of Imaging. 2015;1(1):60-84 www.mdpi.com/journal/jimaging
[14] Erturk M. De-noising MRI using spectral subtraction. IEEE Transaction on Bio-Medical Engineering. 2013;60(6)
[15] Bourne R. Image filters. In: Fundamentals of Digital Imaging in Medicine. Springer London; 2010
[16] Bovik A. Handbook of Image and Video Processing. New York: Academic; 2000
[17] Patel K, Mewada H. A review on different image de-noising methods. International Journal on Recent and Innovation Trends in Computing and Communication. 2014;2(1): 155-159
[18] Baselice F, Ferraioli G, Pascazio V. A Bayesian approach for relaxation times estimation in MRI.MagnReson Imaging.
2016;34(3):312–25
[19] Descombes X, Kruggel F, von Cramon DY. fMRI signal restoration using a spatio-temporal markov random fieldpreserving transitions. NeuroImage. 1998;8(4):340–9.
[20] H. Chen, Y. Zhang, M. K. Kalra, F. Lin, Y. Chen, P. Liao, J. Zhou, and G. Wang, “Low-dose CT with a residual encoder-decoder convolutional neural network,” IEEE Trans. Med. Imaging, vol. 36, no. 12, pp. 2524– 2535, 2017.
[21] Q. Yang, P. Yan, Y. Zhang, H. Yu, Y. Shi, X. Mou, M. K. Kalra, and G. Wang, “Low dose CT image denoising using a generative adversarial network with wasserstein distance and perceptual loss,” arXiv . [39] H. Shan, Y. Zhang, Q. Yang, U. Kruger, W. Cong, and G. Wang, “3D convolutional encoder-decoder network for low-dose CT via transfer learning from a 2D trained network,” arXiv preprint arXiv:1802.05656, 2018. preprint arXiv:1708.00961, 2017.
[22] J. M. Wolterink, T. Leiner, M. A. Viergever, and I.Iˇsgum, “Generative adversarial networks for noise reduction in low-dose CT,” IEEE Trans. Med. Imaging, vol. 36, no. 12, pp. 2536–2545, 2017
[23] W. Yang, H. Zhang, J. Yang, J. Wu, X. Yin, Y. Chen, H. Shu, L. Luo, G. Coatrieux, Z. Gui et al., “Improving low-dose ct image using residual convolutional network,” IEEE Access, vol. 5, pp. 24698–24705, 2017.
[24] E. Kang, J. Min, and J. C. Ye, “A deep convolutional neural network using directional wavelets for low-dose x-ray ct reconstruction,” arXiv preprint arXiv:1610.09736, 2016.
[25] L. Cattell, G. Platsch, R. Pfeiffer, J. Declerck, J. A. Schnabel, C. Hutton, A. D. N. Initiative et al., “Classification of amyloid status using machine learning with histograms of oriented 3d gradients,” NeuroImage: Clinical, vol. 12, pp. 990–1003, 2016.
[26] X. Cao, J. Yang, Y. Gao, Q. Wang, and D. Shen, “Region-adaptive deformable registration of ct/mri pelvic images via learning-based image synthesis,” IEEE Trans. Image Process., 2018.

Tianjin Daxue Xuebao (Ziran Kexue yu Gongcheng Jishu Ban)/
Journal of Tianjin University Science and Technology
ISSN (Online): 0493-2137
E-Publication: Online Open Access
Vol:54 Issue:04:2021
DOI 10.17605/OSF.IO/G3678

[27] S. Wang, M. Kim, G. Wu, and D. Shen, “Scalable high performance image registration framework by unsupervised deep feature representations learning,” in Deep Learning for Medical Image Analysis. Elsevier, 2017, pp. 245–269.
[28] W. Zhang, R. Li, H. Deng, L. Wang, W. Lin, S. Ji, and D. Shen, “Deep convolutional neural networks for multi-modality isointense infant brain image segmentation,” NeuroImage, vol. 108, pp. 214–224, 2015.
[29] H. Chen, Y. Zhang, M. K. Kalra, F. Lin, Y. Chen, P. Liao, J. Zhou, and G. Wang, “Low-dose CT with a residual encoder-decoder convolutional neural network,” IEEE Trans. Med. Imaging, vol. 36, no. 12, pp. 2524– 2535, 2017.
[30] I. Goodfellow, J. Pouget-Abadie, M. Mirza, B. Xu, D. Warde-Farley, S. Ozair, A. Courville, and Y. Bengio, “Generative adversarial nets,” in Proc. Adv. Neural Inf. Process. Syst., 2014, pp. 2672–2680.
[31] M. Arjovsky, S. Chintala, and L. Bottou, “Wasserstein GAN,” arXiv preprint arXiv:1701.07875, 2017
[32] Chenyu You, Qingsong Yang, Hongming Shan, Lars Gjesteby, Guang Li, ShenghongJu, Zhuiyang Zhang, Zhen,” Structurally-sensitive Multi-scale Deep Neural Network for Low-Dose CT Denoising,” IEEE Access, Vol.6, 2020.
[33] Z. Wang, A. C. Bovik, H. R. Sheikh, and E. P. Simoncelli, “Image quality assessment: from error visibility to structural similarity,” IEEE Trans. Image Process., vol. 13, no. 4, pp. 600–612, 2004.
[34] Q. Yang, P. Yan, Y. Zhang, H. Yu, Y. Shi, X. Mou, M. K. Kalra, and G. Wang, “Low dose CT image denoising using a generative adversarial network with wasserstein distance and perceptual loss,” arXiv preprint arXiv:1708.00961, 2017.
[35] J. M. Wolterink, T. Leiner, M. A. Viergever, and I.Ĭsgum, “Generative adversarial networks for noise reduction in low-dose CT,” IEEE Trans.Med.Imaging, vol. 36, no. 12, pp. 2536–2545, 2017.
[36] H. Zhao, O. Gallo, I. Frosio, and J. Kautz, “Loss functions for image restoration with neural networks,” IEEE Trans. Comput.Imaging, vol. 3, no. 1, pp. 47–57, 2017.
[37] https://www.med.upenn.edu/sbia/brats2017/data.html